Comparative assessment of plasmid and oligonucleotide DNA substrates in measurement of *in vitro* base excision repair activity

Esther W. Hou, Rajendra Prasad, Kenjiro Asagoshi, Aya Masaoka and Samuel H. Wilson*

Laboratory of Structural Biology, National Institute of Environmental Health Sciences, National Institutes of Health, 101 T.W. Alexander Drive, Research Triangle Park, NC 27709, USA

ABSTRACT

Mammalian base excision repair (BER) is mediated through at least two subpathways designated 'single-nucleotide' (SN) and 'long-patch' (LP) BER (2-nucleotides long/more repair patch). Two forms of DNA substrate are generally used for *in vitro* BER assays: oligonucleotide- and plasmid-based. For plasmid-based BER assays, the availability of large quantities of substrate DNA with a specific lesion remains the limiting factor. Using sequence-specific endonucleases that cleave only one strand of DNA on a double-stranded DNA substrate, we prepared large quantities of plasmid DNA with a specific lesion. We compared the kinetic features of BER using plasmid and oligonucleotide substrates containing the same lesion and strategic restriction sites around the lesion. The K_m for plasmid DNA substrate was slightly higher than that for the oligonucleotide substrate, while the V_{max} of BER product formation for the plasmid and oligonucleotide substrates was similar. The catalytic efficiency of BER with the oligonucleotide substrate was slightly higher than that with the plasmid substrate. We conclude that there were no significant differences in the catalytic efficiency of *in vitro* BER measured with plasmid and oligonucleotide substrates. Analysis of the ratio of SN BER to LP BER was addressed using cellular extracts and a novel plasmid substrate.

INTRODUCTION

To understand cellular responses to endogenous genotoxic stress, it is important to have insight into the DNA repair process known as base excision repair (BER). BER is involved in repairing base lesions and single-strand breaks that occur thousands of times during the average mammalian cell cycle (1–3) and is generally considered to involve two subpathways defined by the size of the repair patch and the enzymes involved (4–7). These subpathways are termed single-nucleotide (SN) BER and long-patch (LP) BER. As these names imply, in SN BER one nucleotide in the damaged strand is excised and replaced (8–11), whereas LP BER excises and replaces several nucleotides in the damaged strand (6,9). LP BER appears to be a backup subpathway in cases where the SN BER system stalls or where the DNA lesion is refractory to the enzymatic steps of the SN BER subpathway (6,9,12–14).

Components of the BER system are constitutively expressed in mammalian cells, but also exhibit widely divergent tissue-specific expression levels plus up- or down-regulation after genotoxic stress and cytokine exposure (15–20). This dynamic regulatory picture suggests the potential for cell type specific differences in cellular capacity for BER and also for differences in relative use of the two BER subpathways, since there are distinct enzymes and accessory factors involved in each (4–7,10,21–25). Methods for characterization of the overall amount and efficiency of BER *in vivo* are limited, and improved methods for quantitative measurement of repair capacity and subpathway choice are needed for studies of extract-mediated BER.

In recent years, research in the BER area has been greatly facilitated through measurements of *in vitro* BER activity using oligonucleotide and plasmid substrates containing a lesion in a defined site and sequence context (4–6,8,10,26). There has been debate, however, on advantages and disadvantages regarding the form of DNA used as substrate, i.e. plasmid versus oligonucleotide. For example, oligonucleotide substrates offer the advantage of relative ease of preparation of large amounts of pure material, and hence the option of preparing *in vitro* reaction mixtures with an excess of DNA substrate. Under this condition, steady-state measurements of repair activity of extracts can be obtained using short incubation periods (e.g. 1 min) and small amounts of

*To whom correspondence should be addressed. Tel: 919 541 3267; Fax: 919 541 3592; Email: wilson5@niehs.nih.gov

protein extract (e.g. 1 µg). On the other hand, use of a plasmid substrate with the same lesion has involved reaction mixtures with only minimal concentrations of substrate DNA, in view of the difficulty of preparing large quantities of plasmid material. This limitation imposes a need for longer incubation periods with higher amounts of protein extract, in order to observe conversion of a significant amount of substrate into product. Such substrate-limiting, or efficiency-based, conditions can complicate interpretation of reaction kinetics. In addition, there are concerns regarding competing enzymatic activities such as nucleases, as well as plasmid substrate impurities that reduce the effective concentration of substrate. Nevertheless, there can be advantages in using plasmid substrate molecules. For example, artifacts due to protein binding to DNA ends can be eliminated. Also plasmids allow assembly of multi-protein complexes that are too large to be accommodated on oligonucleotide molecules. In addition, plasmids enable use of clamp proteins requiring long and/or circular substrate molecules, such as PCNA (23). Finally, there has been a suggestion that plasmid DNA substrates are more relevant to *in vivo* events than oligonucleotide substrate molecules, however, this latter point has been controversial.

Resolution of this debate and uncertainties about choice of substrate DNA can be facilitated by a direct comparison of BER kinetics obtained with each type of DNA bearing the same lesion and sequence context. This comparison has been enabled recently by the introduction of a method for plasmid DNA preparation that yields large amounts of purified plasmid in a relatively short period (26–30). In the present study, we examined cell extract-mediated uracil-initiated BER using plasmid and oligonucleotide substrates with the U:G mispair in the same sequence context. Repair was measured under steady-state conditions for each type of substrate. Values for K_m and V_{max} were obtained using laboratory reference extracts from bovine testis and mouse embryonic fibroblasts (MEF). The results of these analyses indicated that plasmid and oligonucleotide substrates yielded similar V_{max} values for uracil-DNA BER activity, although the catalytic efficiency (V_{max}/K_m) of repair with the oligonucleotide substrate was slightly higher than with the plasmid substrate. Methods for measuring the ratio of the two BER subpathways, SN BER and LP BER, and for evaluation of the LP BER repair patch size are also discussed.

MATERIALS AND METHODS

Materials

Synthetic oligodeoxyribonucleotides were from Integrated DNA Technologies, Inc. (Coralville, IA, USA) and Oligos Etc. Inc. (Wilsonville, OR, USA). The [α-^{32}P]dCTP and dTTP (3000 Ci/mmol) were from GE HealthCare (Piscataway, NJ, USA). *Pfu* DNA polymerase was from Stratagene (La Jolla, CA, USA). Endonuclease *N.Bst*NB1, T4 DNA ligase and all other restriction enzymes were from New England Biolabs (Beverly, MA, USA). Plasmids were isolated using Qiagen Plasmid Maxi kits from Qiagen

(Valencia, CA, USA). Streptavidin-coated magnetic beads (Dynabeads M-280) were from Invitrogen (Carlsbad, CA, USA). Recombinant human DNA polymerase β (Pol β) was overexpressed and purified as described previously (31). Human uracil-DNA glycosylase (UDG), apurinic/apyrimidinic endonuclease (APE) and DNA ligase I were purified as described previously (32–34).

Preparation of lesion-specific plasmid DNA substrates

Lesion-specific BER plasmid substrates were prepared essentially as described previously (29) with slight modifications. Plasmid pUC19N was derived from pUC19 by inserting a 43-bp phosphorylated oligonucleotide (5′-GATCGAGTCGAATGCATGCCTCGAGTCT A GAGGTACCAGATCT-3′) at the *Bam*HI site position 417. During this process the *Bam*HI site was lost. The resulting pUC19N contained two *N.Bst*NB1 sites flanking 48 bases that could be substituted with a lesion-specific oligonucleotide. The sequence of the pUC19N plasmid was confirmed by sequencing. A 48-mer oligonucleotide in the sense strand that contained a defined lesion base [uracil or tetrahydrofuran (THF) at position 20, underscored C above] was replaced between two *N.Bst*NB1 sites as follows: pUC19N (100 µg, 57 pmol) was digested with 500 U of *N.Bst*NB1 at 55°C for 2 to 3 h, followed by subsequent incubation with 200 pmol 3′-biotin-tagged complementary 48-mer oligonucleotide on a rotary shaker for 30 min at 37°C. Then, streptavidin-coated Dynabeads M-280 (400 pmol), pre-equilibrated with 10 mM Tris–HCl, pH 7.5, 0.5 mM EDTA and 1 M NaCl, were added to the reaction mixture, and the mixture was incubated for 2 h at 37°C. The 48-bp biotin-tagged DNA, adsorbed onto magnetic beads, was separated from the gapped-pUC19N DNA by placing the reaction mixture tube on a magnet for 2 min to collect the beads. The supernatant was carefully removed with a pipette while the tube remained on the magnet. Gapped-plasmid DNA in the supernatant was extracted twice with phenol/chloroform and precipitated with 95% ethanol. A 20-fold excess of uracil or THF lesion-containing 48-mer oligonucleotide (1.0 nmol) was added to the gapped-pUC19N DNA in 10 mM Tris–HCl, pH 8.0 and 50 mM NaCl. The DNA mixture was annealed at 45°C for 4 h, and then incubated at 25°C for 15 h with 5000 U of T4 DNA ligase. In order to purify the closed-circular DNA (ccDNA) plasmid from the un-ligated nicked DNA, two rounds of isopycnic centrifugation in CsCl$_2$ with ethidium bromide were performed. The yield of lesion-specific plasmid DNA was ∼30–50% of the starting plasmid (i.e. ∼25 pmol). The purity of each plasmid preparation was evaluated by digestion with *Xho*I and subsequent electrophoretic separation of ccDNA and linearized DNA. In this assay, the starting plasmid, pUC19N (plasmid without a lesion), was linearized by *Xho*I digestion, whereas the lesion-specific substrates were not. This test for contaminating starting plasmid was considered an important precaution as contamination with the starting plasmid was found to be significant for some preparations, owing to inefficient removal of 48-mer *N.Bst*NB1 DNA fragment and religation in the last

step described above. The resulting plasmids containing either uracil or THF were designated as pUN1 or pUN2, respectively. Routinely, the ratio of lesion-specific plasmid to starting plasmid was greater than 3:1 in the experiments shown here.

Preparation of lesion-specific oligonucleotide DNA substrates

Unphosphorylated 55-mer oligonucleotide (100 mM) with 3′ inverted dT (5′-TCGGTACCCGGGGATCGAGT CGAATGCATGCCTCGAGTCTAGAGGTACCAGAT CT-3′) containing either uracil or THF at position 32 (underscored C) was annealed to its complementary unphosphorylated 55-mer in 10 mM Tris–HCl, pH 8.0 and 100 mM NaCl, and then the DNA solution was diluted to 1 mM in the same buffer. The solution was divided into aliquots and stored at −80°C.

Preparation of lesion-specific pPAL1 plasmid

The plasmid pGL4.10TKΔKpn (5.0 kb) was constructed from pGL4.10 (Promega, Madison, WI, USA) by inserting the TK promoter between *Kpn*I and *Hind*III sites. During this process the *Kpn*I site was lost. For the *in vitro* BER plasmid assay, pPAL1 was prepared by replacing the *Hind*III-*Apa*I fragment of pGL4.10TKΔKpn with an oligonucleotide that contained a uracil at a new *Kpn*I site and unique *Nco*I and *Sac*I restriction sites.

To prepare the *Hind*III-*Apa*I fragment, pGL4.10TK ΔKpn was digested with *Apa*I and subsequently treated with calf intestine alkaline phosphatase. The resultant plasmid was digested by *Hind*III and purified by 1% agarose gel electrophoresis. Then a 73/81-bp hybrid oligonucleotide was prepared by annealing unphosphorylated 73-mer 5′CTTCTTAATGTTTTTGGCATCTTCC ATGGTGGCTTTACCAAGGTAUCAGTAAGTATTA ATTAAGGAGAGCTCA-3′ and 5′-phosphorylated 81-mer 5′-AGCTTGAGCTCTCCTTAATTAATACTT ACTGGTACCTTGGTAAAGCCACCATGGAAGATG CCAAAAACATTAAGAAGGGCC-3′ DNA. Ligation of this oligonucleotide into the *Hind*III-*Apa*I digestion product of pGL4.10TKΔKpn was carried out as described (35). The closed circular DNA was separated by 1% low-melting temperature agarose gel electrophoresis containing SYBR Gold nucleic acid gel stain (Invitrogen), and the plasmid was recovered using a gel extraction kit (Qiagen). The resulting plasmid, pPAL1, was obtained in microgram quantities.

Nuclear extract preparation

Nuclear extract was prepared from bovine testis essentially as described previously (36). Briefly, 100 g of bovine testis was minced in 300 ml buffer A [10 mM Hepes, pH 8.0, 1.5 mM MgCl$_2$, 10 mM NaCl, 0.5 mM dithiothreitol (DTT), 10 mM sodium metabisulfite, 0.1 mM 4-(2-aminoethyl)benzenesulfonylfluoride (AEBSF), 1 mM benzamidine, 1 μg/ml leupeptin and 1 μg/ml pepstatin A] and homogenized using four 10 s bursts with a blender at 4°C. The homogenate was pelleted by centrifugation at 10 000 × g for 10 min at 4°C. Pellet fraction was resuspended in 150 ml of buffer B (same as buffer A, except it contained 1 M NaCl) and blended using three

5 s bursts. The homogenate was centrifuged at 100 000 × g for 1 h at 4°C. The clear supernatant fraction was brought to 40% saturation by adding solid ammonium sulfate slowly with stirring; stirring was continued for 1 h at 4°C. The precipitate was recovered by centrifugation at 14 000 × g for 20 min at 4°C. The pellet fraction was resuspended in 50 ml of buffer C (25 mM Hepes, pH 7.5, 100 mM NaCl, 1 mM DTT, 10 mM sodium metabisulfite, 0.5 mM EDTA, 0.1 mM AEBSF, 1 mM benzamidine, 1 μg/ml leupeptin, 1 μg/ml pepstatin A and 20% glycerol) and dialyzed against the same buffer. The dialyzed nuclear extract was clarified by centrifugation at 10 000 × g for 20 min. The clear supernatant fraction was referred to as the bovine testis nuclear extract (BTNE) and stored at −80°C. Protein concentration was determined with a Bio-Rad protein assay kit using bovine serum albumin (BSA) as a standard.

Cell extract preparation

Whole cell extract was prepared as previously described (4). Briefly, cells were washed twice with phosphate-buffered saline at room temperature, detached by scraping, pelleted by centrifugation and resuspended in Buffer I (10 mM Tris–HCl, pH 7.8, 200 mM KCl and protease inhibitor cocktail). An equal volume of Buffer II (10 mM Tris–HCl, pH 7.8, 200 mM KCl, 2 mM EDTA, 40% glycerol, 0.2% Nonidet P-40, 2 mM DTT and protease inhibitor cocktail) was added. The suspension was rotated for 1 h at 4°C, and the resulting extract was clarified by centrifugation at 14 000 rpm at 4°C. The protein concentration of the extract was determined as above, and aliquots were stored at −80°C.

In vitro BER assay

Uracil- and THF-containing plasmids were designed as described above to quantify total BER, SN BER and LP BER in the same reaction. A 48-nt *N.Bst*NB1 fragment containing uracil or THF (Figure 1) was inserted in pUC19, which upon digestion with strategic restriction enzymes, as indicated in Figure 2, would generate fragments representing total BER product (41-bp *Kpn*I fragment), SN BER plus LP BER (25-bp *Kpn*I-*Xho*I fragment) and LP BER (16-bp *Xho*I-*Kpn*I fragment). BER assays were performed using reaction mixtures of 10 μl final volume that contained 20–500 nM plasmid or oligonucleotide DNA substrate, 10 μg of extract, 50 mM Tris–HCl, pH 7.5, 5 mM MgCl$_2$, 20 mM NaCl, 1 mM DTT, 4 mM ATP, 20 μM each of dATP, dGTP and dTTP or dCTP and 2.3 μM [α-^{32}P]dCTP or [α-^{32}P]dTTP, as indicated. The incubation was at 37°C for 1 to 30 min, as indicated. Reactions were terminated by adding 1 μl of 0.5 M EDTA and 90 μl TE (10 mM Tris–HCl, pH 8.0 and 1 mM EDTA), and this was followed by phenol/chloroform extraction and ethanol precipitation. To facilitate ethanol precipitation, 100 ng of carrier tRNA was added to each reaction mixture. The resulting DNA pellet fraction was dissolved in H$_2$O and divided into three equal portions. These DNA-containing portions were subjected to restriction enzyme digestion as follows: (i) no enzyme, (ii) *Kpn*I and (iii) *Kpn*I plus

*Xho*I. The reaction mixtures were incubated for 90 min at 37°C. The resulting reaction products were separated by 20% denaturing polyacrylamide gel electrophoresis (PAGE). The gels were dried, scanned with a Typhoon PhosphorImager and the data were analyzed with ImageQuant software. The BER assay, with uracil-containing plasmid, pPAL1, also was performed under similar reaction conditions as above, and the repaired DNA was restricted with *Nco*I/*Sac*I and/or *Kpn*I, as indicated in Figure 5. The experiments were repeated several times, and representative images and average values of SN BER and LP BER are shown. *In vitro* BER assays using the 55-bp oligonucleotide duplex DNA and cellular extracts were performed under similar reaction conditions as with the plasmid DNA.

RESULTS

Preparation of plasmid DNA substrates

A plasmid DNA substrate containing either uracil or THF opposite guanine was prepared as outlined in Figure 1. Uracil opposite guanine was chosen because this mismatch is a widely used initiating lesion for studies of *in vitro* BER. The THF abasic site lesion was chosen as a reference because all BER with this lesion occurs through the LP BER subpathway, since DNA ligation after the gap-filling step in BER is blocked by the persistent THF group (12,13). A key feature in plasmid preparation was the use of the single-strand cutting restriction enzyme *N.Bst*NB1, such that a single-strand gap of 48 nt was introduced into the plasmid and the released 48-mer was removed (Figure 1, see penultimate step). Eventually, a synthetic 48-mer uracil-containing or THF-containing oligonucleotide was annealed into the gap, and the nicks were ligated with good yield (Figure 1, final step). The plasmids (pUN1 or pUN2) thus prepared could be purified in milligram quantities, enabling the use of as much as micromolar final concentrations of plasmid substrate in BER reaction mixtures.

In addition, these plasmids were designed such that the lesion was flanked with two *Kpn*I sites (Figure 2A). Digestion of BER reaction products with this enzyme yielded a 41-nt fragment (41-mer). Upon denaturing gel electrophoresis, the incorporation of labeled dNMPs into the repair patch within this fragment could be measured. Quantitative assessment of the repair product formed during the BER incubation could be obtained by double digestion with *Kpn*I and *Xho*I and use of ^{32}P-labeled dCTP as one of the nucleotide substrates. In this way, incorporation of labeled dCMP into the first dNMP position of the repair patch was used to quantify the molar amount of repair product formed. This digestion also produced a 16-mer fragment corresponding to the second through seventeenth incorporations by the LP BER subpathway, and should contain most of the LP BER product (Figure 2A). In some cases, *Kpn*I digestion alone yielded a 25-nt (25-mer) labeled fragment reflecting accumulation of stalled/unligated BER intermediate, i.e. intermediate prior to the DNA ligation step in SN BER or the strand displacement step in LP BER. In the experiments shown
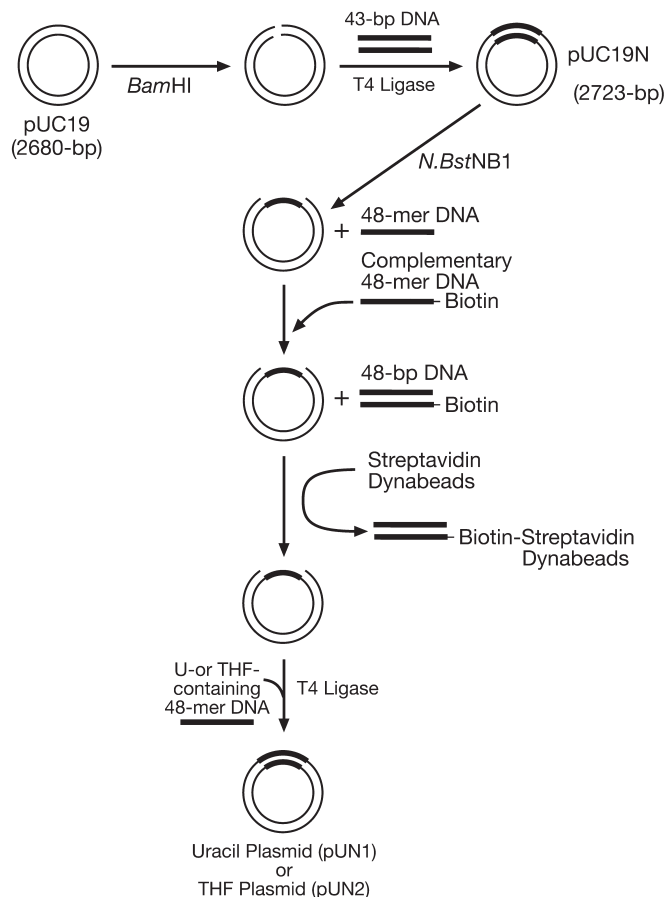
Figure 1. Construction of lesion-specific plasmid substrates. Lesion-specific plasmid substrates for *in vitro* BER assays, pUN1 and pUN2, were constructed as described under 'Materials and Methods section'. The pUC19 was cut with *Bam*HI and a 43-bp fragment was inserted to create pUC19N that contained two *N.Bst*NB1 sites. Then, the pUC19N was digested with *N.Bst*NB1 to generate a 48-nt gap. The 48-nt fragment was removed by hybridization to a biotinylated-tagged complementary oligonucleotide and followed by adsorption onto streptavidin-coated magnetic beads. Next, the plasmid, pUN1 or pUN2, was created by re-hybridization and ligation of gapped pUC19N to the 5′-phosphorylated 48-mer oligonucleotide containing either uracil or THF, respectively, as shown.

subsequently, this material was considered as background since it did not represent complete repair. Digestion with other restriction enzymes is also illustrated in Figure 2. Two fragments are produced by double digestion with *Xho*I and *Xba*I, a 6-mer representing the second through seventh incorporations in the repair patch and a 23-mer representing incorporations out to the 30th position in the repair patch (Figure 2A).

With the oligonucleotide substrates, a related strategy was used for analysis of BER reaction products. These oligonucleotide substrates had lesions and sequences identical to those in the plasmid substrates (Figure 2). In the case of products formed in reaction mixtures with labeled dCTP, digestion with *Xho*I yielded a 32-mer containing the first labeled dCMP incorporated (Figure 2B), allowing assessment of the molar amount of product formed. The stalled or unligated BER

A Plasmid Substrate
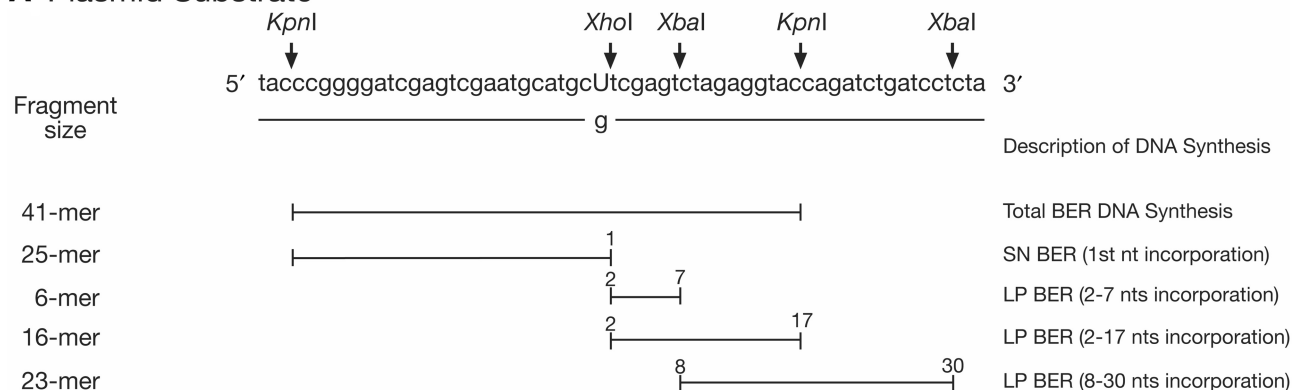
B Oligonucleotide Substrate
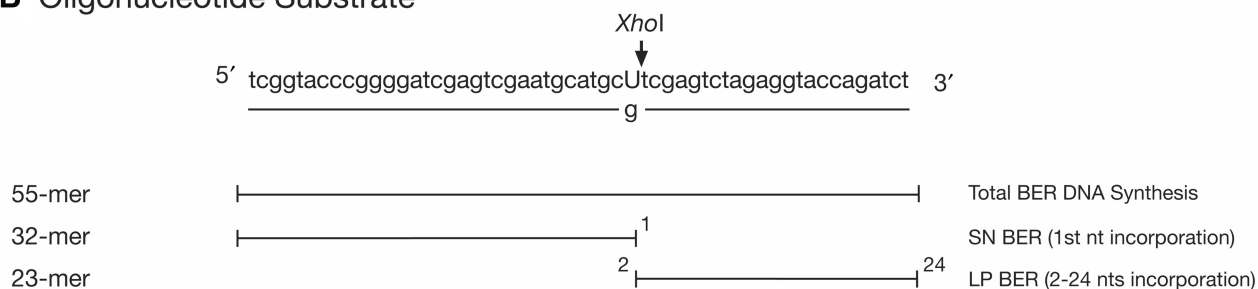
Figure 2. Schematic representation of plasmid and oligonucleotide DNA substrates. (**A**) Sequence of the uracil-containing fragment of pUN1 and restriction sites are shown. After the repair reaction, DNA products were restricted with the indicated enzymes, and fragments were separated by 20% denaturing PAGE. DNA fragment sizes and descriptions of DNA synthesis products are indicated. (**B**) The sequence of 55-bp oligonucleotide containing uracil at position 32 and a strategic restriction site is shown. The sequence of the oligonucleotide substrate is identical to the 41-mer fragment of plasmid in (A). DNA fragment sizes and descriptions of DNA synthesis products are indicated.

intermediate was observed in some cases, and again, this material was considered as background. The *Xho*I digestion also yielded a 23-mer fragment containing the LP BER incorporations (Figure 2B).

Typical results obtained with a laboratory reference tissue extract, BTNE, and the plasmid and oligonucleotide substrates described above are shown in Figure 3. Repair of the uracil-DNA plasmid substrate and digestion with *Kpn*I resulted in the labeled 41-mer fragment; very little stalled 25-mer intermediate was observed (Figure 3A). In contrast, with the THF-containing plasmid substrate, a significant band representing the stalled intermediate was observed with *Kpn*I digestion alone (Figure 3A). This indicated accumulation of the intermediate at the step just prior to strand displacement synthesis in LP BER. The results obtained with the oligonucleotide substrates without restriction enzyme digestion were similar, except the stalled intermediate was more abundant (Figure 3B).

Double digestion of the plasmid products yielded the 25-mer and 16-mer fragments described above (Figure 3C). The results illustrated that most of the uracil-DNA repair corresponded to SN BER, as expected from earlier results (9). Analysis of the product formed on the THF-containing oligonucleotide substrate revealed that the amount of stalled intermediate was greater than

the LP BER product, and with uracil-DNA the results were similar to those with plasmid substrate (Figure 3D).

Comparison of steady-state kinetic features of repair with plasmid and oligonucleotide substrates

The main goal of this study was to compare kinetic features of BER product formation with plasmid and oligonucleotide substrates. We measured the initial rates of BTNE-mediated BER for the two forms of substrate under conditions of substrate excess. The rates of product formation with various uracil-DNA substrate concentrations were linear over the first 10 min of incubation, as illustrated at one substrate concentration in the experiment shown in Figure 4. Kinetic features for BTNE-mediated BER with the two substrates are summarized in Table 1. The maximal velocities (V_{max}) of BER product formation for the plasmid and oligonucleotide substrates were similar, but the K_m for the plasmid substrate, pUN1, was slightly higher than that for the oligonucleotide substrate. The resultant efficiency (V_{max}/K_m) was slightly higher (3-fold) with the oligonucleotide substrate. These results indicate that similar rates of uracil-DNA repair can be obtained with the two forms of substrate, especially when they are used at concentrations high enough to support near maximal synthesis, i.e. $\gg K_m$.
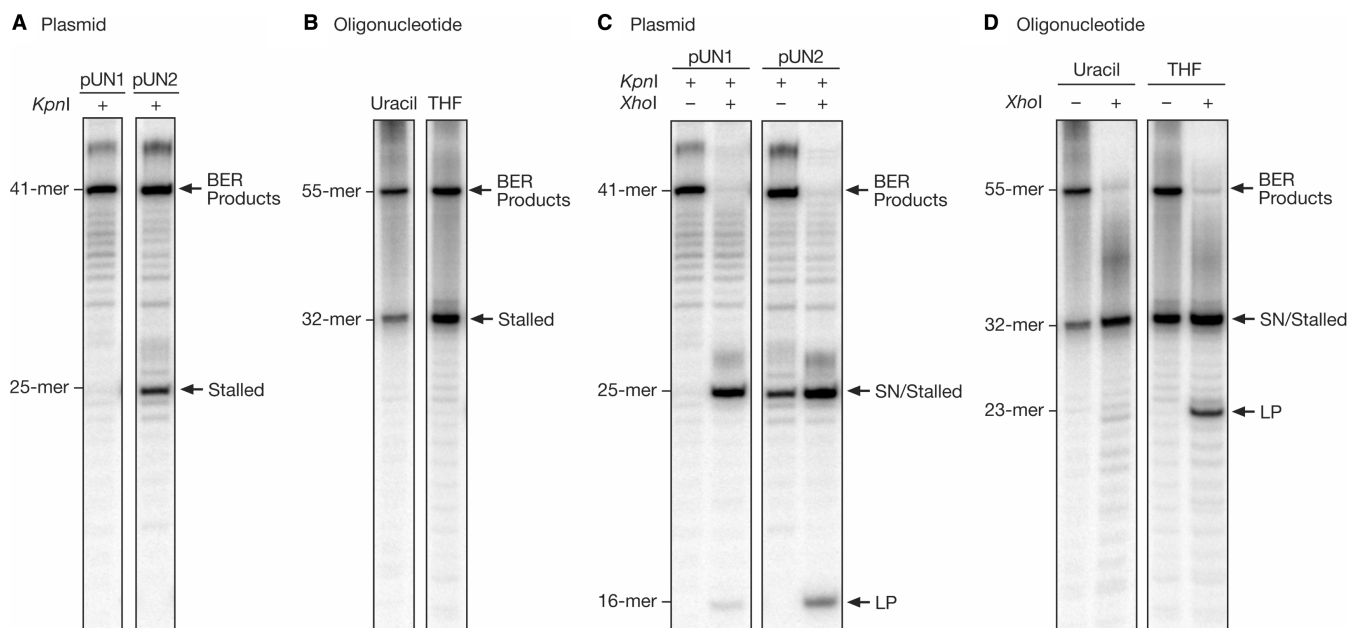
Figure 3. Comparison of BER reaction products using plasmid and oligonucleotide substrates. In order to compare the BER reaction products using plasmid-based or oligonucleotide-based assay, the repair reaction was performed with lesion-specific DNA substrate, as indicted at the top of each panel, and BTNE. The reaction conditions and product analyses were as described under 'Materials and Methods' section. Panels (**A**–**D**), BER reaction was performed in a 10 μl reaction mixture that contained 50 nM plasmid/oligonucleotide DNA (uracil- or THF-containing DNA) and 10 μg BTNE. Incubation was for 30 min at 37°C. The reaction products were purified, digested with the indicated restriction enzyme (s), and then separated by 20% denaturing PAGE. Panels (A) and (B) show the total BER products represented by 41-mer and 55-mer DNA fragments obtained with uracil or THF-containing plasmid, pUN1 or pUN2, and oligonucleotide substrates, respectively. The 25-mer and 32-mer DNA fragments observed with plasmid and oligonucleotide substrates, respectively, represented unligated or stalled intermediates. Panels (C) and (D), the remaining reaction products in (A) and (B) were digested with *Kpn*I or *Kpn*I plus *Xho*I (Panel C), and *Xho*I (Panel D), respectively. This resulted in 25-mer (SN BER) and 16-mer (LP BER) DNA fragments from plasmid substrate and 32-mer (SN BER) and 23-mer (LP BER) DNA fragments from oligonucleotide substrate, respectively. In cases where unligated or stalled intermediates were observed (i.e. the 25-mer and 32-mer fragments), the counts in these molecules were considered as background and subtracted for the calculation of SN BER. The positions of total BER, SN BER/stalled and LP BER products are indicated.

Use of plasmid substrate in measurement of the ratio of SN to LP BER

In some cases, it is desirable to measure the relative amounts of the SN and LP BER subpathways. Adjusting the sequence of the repair patch to eliminate ambiguity from incorporation of more than one labeled dNMP in each subpathway can facilitate this measurement. To accomplish this type of measurement, we constructed an alternate plasmid substrate termed 'pPAL1' (Figure 5A). This plasmid was designed for use in BER assays along with [α-^{32}P]dCTP as the labeled nucleotide substrate. To illustrate use of this method, incubations were conducted with MEF extract. Double digestion of the reaction product with *Nco*I and *Sac*I yielded a 47-mer representing the entire excision repair patch and a small amount of stalled intermediate (Figure 5B). Digestion with these enzymes plus *Kpn*I yielded a 22-mer with the first dNMP incorporated, labeled dCMP, and a 25-mer with labeled dCMP corresponding to the second nucleotide incorporated and potentially the 25th dCMP incorporated into the repair patch (Figure 5A). Since the repair patch in LP BER is shorter than 25 residues, potential dCMP incorporation at the 25th position can be ignored. Therefore, quantification of [α-^{32}P]dCMP incorporated into the 22-mer and 25-mer fragments, respectively, yields

the molar amounts of total BER product (SN and LP BER) and LP BER product, as illustrated in Figure 5. In this case, the ratio of SN BER to LP BER was approximately 60:40 (Figure 5C), as expected from earlier results obtained by different methods (21,37).

Repair patch analysis for long patch base excision repair products

As noted in Figure 2, the plasmid and oligonucleotide substrates can be used for repair patch size assessment of LP BER reaction products. Such analysis involves restriction enzyme digestion and then the electrophoretic separation and quantification of various labeled fragments (^{32}P-labeled dNMP incorporation). Typical results from this type of analysis are illustrated in Figure 6. In the experiment shown, we used the THF-containing plasmid, pUN2, (Figure 1) so that repair corresponded to the LP BER subpathway only, along with an extract known to be proficient in LP BER (i.e. from MEFs). Measurement of dCMP and dTMP incorporated in separate incubations was conducted (Figure 6). In this case for LP BER, the amount of dCMP incorporation into the first dNMP position (i.e. 25-mer) is equal to the amount of dTMP incorporation into the second dNMP position. Therefore, to evaluate LP BER synthesis beyond the second
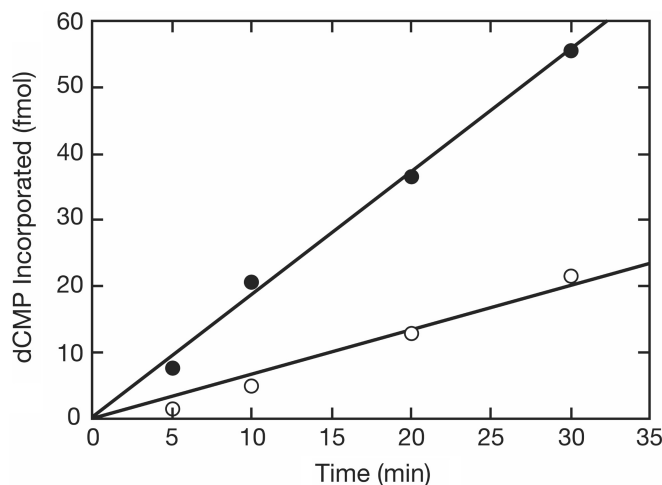
Figure 4. Steady-state kinetic analysis of the repair reaction using plasmid and oligonucleotide substrates. The reaction conditions and products analyses were as described under 'Materials and Methods section'. Repair reaction was performed under conditions of substrate excess with BTNE using either uracil-containing plasmid (open circle) or uracil-containing oligonucleotide (closed circle) substrate. The concentrations of plasmid and oligonucleotide substrates were 450 nM and 200 nM, respectively. Aliquots were taken at the indicated time intervals, and the DNA products were analyzed as in Figure 3. Time courses of product formation for the plasmid and oligonucleotide substrates are shown. BER products were quantified with ImageQuant software, and the data were fitted to a straight-line equation. The initial rates of BTNE-mediated BER for the plasmid and oligonucleotide substrates were 0.67 and 1.85 fmol dCMP incorporated/min, respectively. The experiments were repeated three times, and a representative graph from one experiment is shown.

nucleotide, the amount of dTMP incorporated into the second position of the 16-mer could be subtracted from total dTMP incorporation into the 16-mer; this synthesis in the 16-mer for dTMP incorporation was similar to that for dCMP incorporation (Figure 6B and C).

Further analysis of repair patch size is illustrated in Figure 7. Typical results (Figure 7A) and the strategy for analysis using ^{32}P-labeled dCMP incorporation (Figure 7B) were as follows: Restriction with *Kpn*I yielded a 41-nt fragment (41-mer) representing repair patch synthesis, i.e. from one up to 17 nucleotide incorporations (Figure 7A, lane 1, and B). With *Kpn*I digestion, some 25-mer BER intermediate was also observed, reflecting stalling at this intermediate. Incorporation of the first nucleotide in the repair patch, dCMP, was measured after double digestion with *Kpn*I and *Xho*I, yielding the 25-mer and the 16-mer (Figure 7A lane 2). The 16-mer fragment reflected three LP BER dCMP incorporations (Figure 7A, lane 2, and B). For LP BER synthesis at the 2nd through 7th nucleotides and longer repair patches, respectively, we measured dCMP incorporation into the corresponding fragments after double digestions with *Xho*I and *Xba*I, i.e. two fragments (6-mer and 23-mer) as illustrated in Figure 7 (Figure 7A, lane 3, and B). Incorporation into the 6-mer was greater than that into the 23-mer, indicating that most of the LP BER corresponded to repair patches of 7 nt or less (Figure 7C).
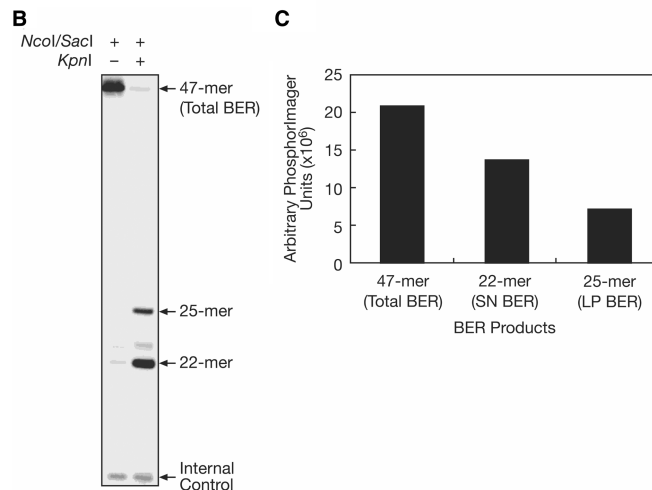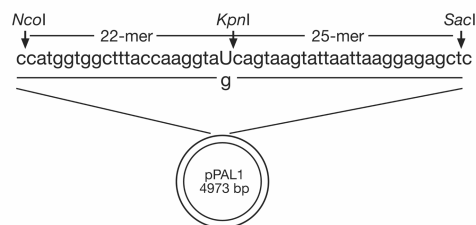
Figure 5. Assessment of the ratio of SN to LP BER after repair incubation. (**A**) Schematic diagram of uracil-containing plasmid, 'pPAL1', is shown. A uracil residue (U) was placed in a central position of the *Nco*I/*Sac*I fragment. Three strategic restriction enzyme sites, *Nco*I, *Kpn*I and *Sac*I, were designed around the lesion such that SN and LP BER could be analyzed in the same repair reaction mixture. After completion of the BER reaction in the presence of [α-^{32}P]dCTP, repair products were restricted with either *Nco*I and *Sac*I or *Nco*I, *Sac*I and *Kpn*I, which generated 47-, 25- and 22-mer DNA fragments representing total, LP and SN BER products, respectively. To calculate SN and LP BER products, counts in the 25-mer fragment were subtracted from the total counts in 22-mer fragment, because for every incorporation of dCMP at the second position, next to uracil, one dCMP will be incorporated first at the lesion site. (**B**) pPAL1 (20 nM) was incubated with 10 μg of MEF extract in 50 mM Tris–HCl, pH 7.5, 5 mM MgCl$_2$, 20 mM NaCl and 1 mM DTT. The reaction was conducted at 37°C for 30 min in the presence of 20 μM each of dATP, dGTP, dTTP and 2.3 μM [α-^{32}P]dCTP. A 16-mer radiolabeled DNA fragment was added in each reaction mixture as an internal control prior to phenol/chloroform extraction and ethanol precipitation. The reaction products were analyzed by 15% denaturing PAGE. The combinations of restriction enzymes used are shown at *top* of the PhosphorImager panel. The description of each radiolabeled band is indicated on the *right-hand* side of the image. (**C**) Quantification of total, SN and LP BER is shown in a bar graph. Band intensity of each radiolabeled DNA fragment, 47-, 25- and 22-mer, was measured in terms of arbitrary PhosphorImager units and plotted as total BER, SN BER and LP BER. The experiments were repeated three times and a PhosphorImage of a representative experiment is shown.

DISCUSSION

We made use of a recently acquired method for obtaining large amounts of plasmid DNA after a preparative *in vitro* ligation step (30). A plasmid with a single-strand 48 base gap was prepared in high yield and in pure enough form to enable annealing a 48-mer lesion-containing oligonucleotide into the gap. After ligation and purification of the

lesion-containing plasmid DNA substrate, a relatively large amount of DNA was available for use in routine BER incubations (Figure 1). The availability of such large quantities of plasmid substrate made it possible for us to compare steady-state kinetic values for BER obtained with an oligonucleotide substrate with those obtained with a plasmid substrate. Such a comparison had been
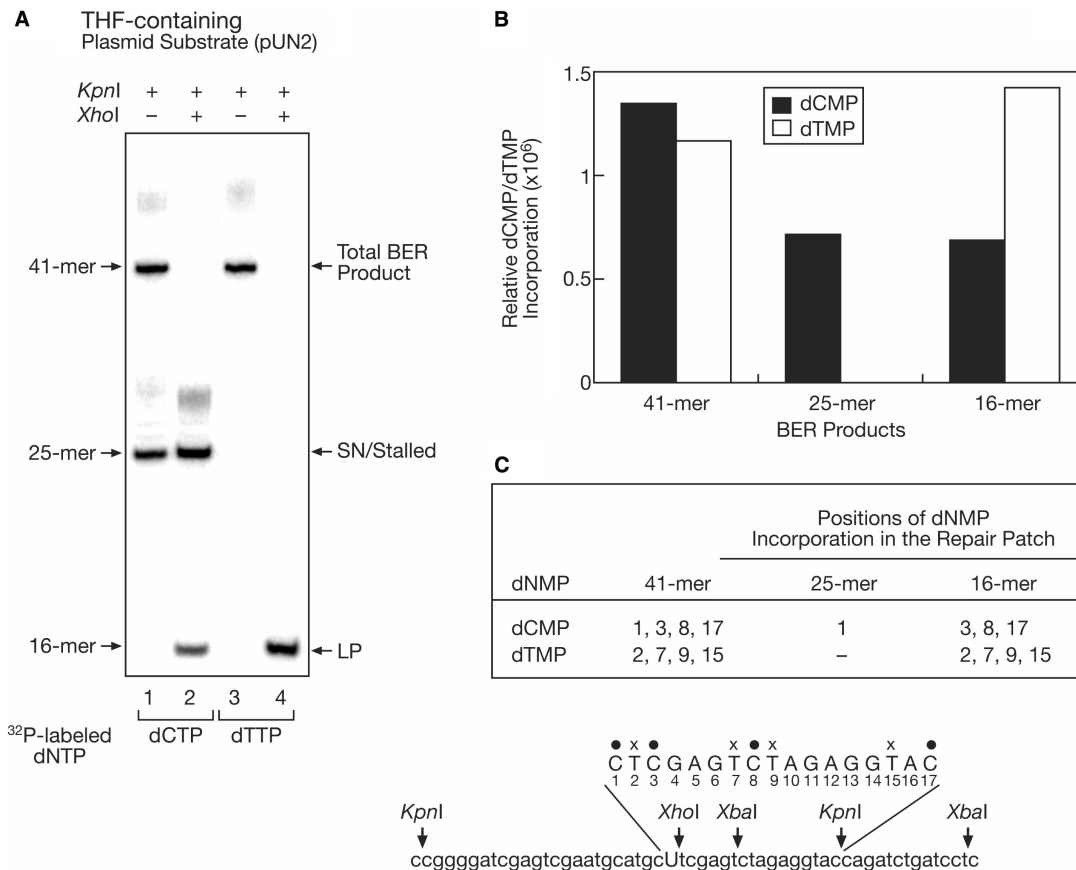
unresolved and remained an important consideration. Some investigators maintained that plasmid substrates are more biologically relevant or useful than oligonucleotide substrates. On the other hand, others have held the opposite viewpoint asserting that plasmid substrates are of limited and specialized use because of the necessity to employ miniscule concentrations of substrate DNA and long incubation periods, both of which potentially confound interpretations on BER capacity measurements. Our results indicated that the two forms of substrate yielded similar values for rates of repair in a nuclear extract, provided the DNA substrate concentration was high enough in the reaction mixture.

A precaution emerged from the observation that K_m for plasmid substrate was higher than K_m for oligonucleotide substrate. An explanation for this difference was not examined. However, on a practical level, when a substrate excess or steady-state approach is used to quantify

Table 1. Steady-state kinetic measurements of BER using plasmid and oligonucleotide substrates

	Oligonucleotide			Plasmid	
K_m (nM)	V_{max} (nM/min)	V_{max}/K_m (min^{-1} × 10^{-4})	K_m (nM)	V_{max} (nM/min)	V_{max}/K_m (min^{-1} × 10^{-4})
51.4 (9.9)	0.05 (0.02)	9.7 (4.3)	216 (27.3)	0.09 (0.03)	4.0 (1.0)

Mean (±SE) of four independent experiments.

Figure 6. Incorporation of labeled dCMP and dTMP into the repair patch produced during LP BER of the THF-containing plasmid. The repair reaction was performed with THF-containing plasmid, pUN2 and MEF extract. The reaction conditions and product analyses were as described under 'Materials and Methods section'. (**A**) BER reaction was performed in a 10 μl reaction mixture that contained 20 nM pUN2, 10 μg MEF extract and either ^{32}P-dCTP (lanes 1 and 2) or ^{32}P-dTTP (lanes 3 and 4). Incubation was for 30 min at 37°C. The reaction products were analyzed as in Figure 3. The restriction enzymes used are shown at the *top* of the PhosphorImager panel. The description of each radiolabeled band is indicated on both sides of the image. (**B**) Quantification of total BER (41-mer), SN BER (25-mer) and LP BER (16-mer) is shown in a bar graph. A small portion of each reaction was spotted on the gel filter for calculations of incorporation of ^{32}P-dCMP or ^{32}P-dTMP in DNA. The band intensity of each radiolabeled DNA fragment, 41-, 25- and 16-mer, was measured in terms of arbitrary PhosphorImager units and then converted into relative dCMP or dTMP incorporation. The experiments were repeated three times, and the PhosphorImage of a representative experiment is shown. (**C**) The positions of dCMP (filled circle) or dTMP (cross) incorporation in the 41-, 25- and 16-mer fragments, and the restriction sites are indicated.
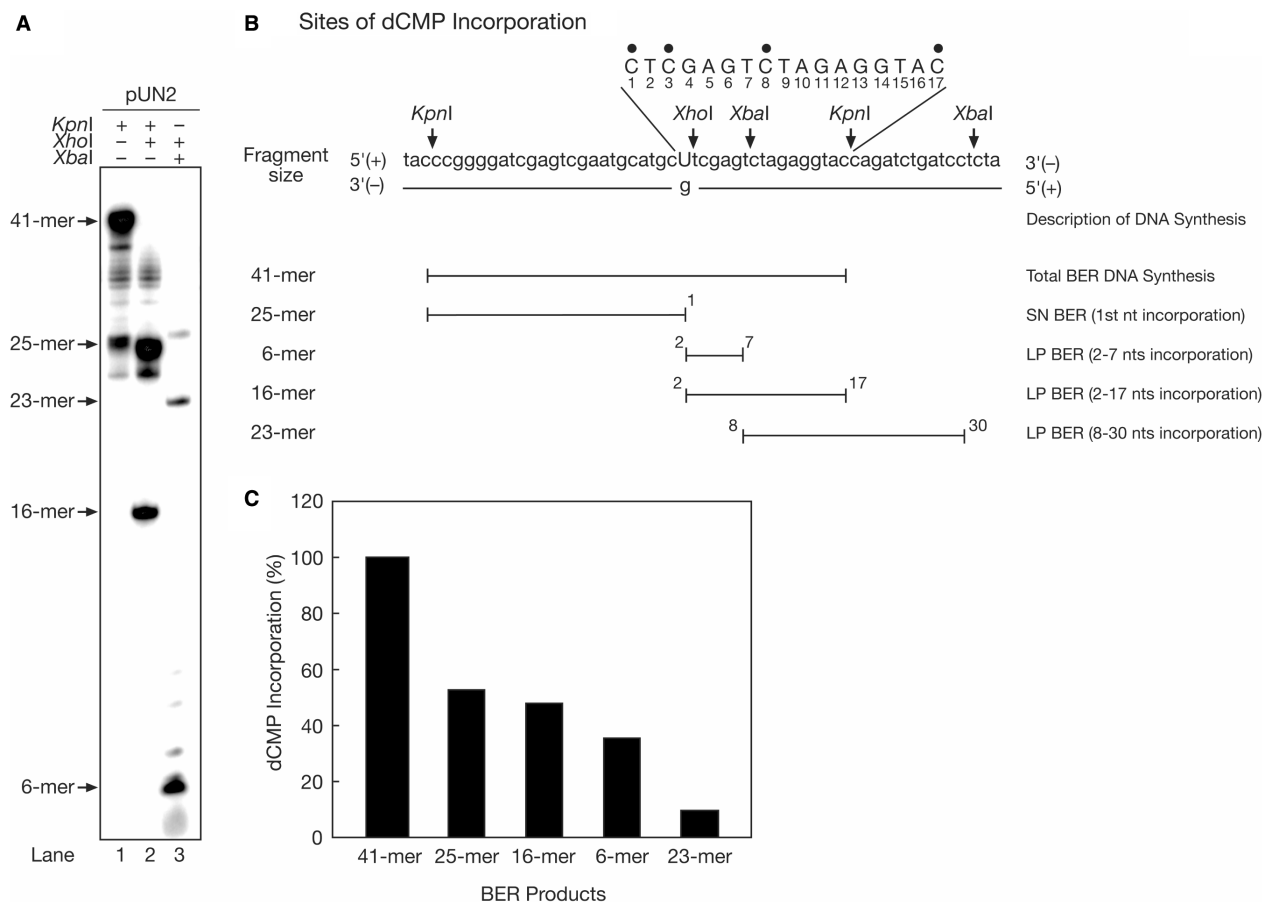
Figure 7. Restriction analysis and quantification of dCMP incorporation into the repair patch produced during LP BER in MEF extract. The repair reaction was performed with THF-containing plasmid, pUN2 and MEF extract. (**A**) BER reaction was performed in a 10 μl reaction mixture that contained 20 nM pUN2, 10 μg MEF extract, and ^{32}P-dCTP. Incubation was for 30 min at 37°C. The reaction products were analyzed as in Figure 3. The restriction enzymes used are shown at the *top* of the PhosphorImager panel. The positions of the restricted DNA fragments are indicated on the *left-hand* side of the image. (**B**) DNA fragment sizes and description of DNA synthesis products are indicated. Sites of dCMP incorporation (filled circle) in the repair patch are indicated. (**C**) The incorporation of dCMP (%) in different BER fragments was plotted in a bar diagram. Conversion of arbitrary PhosphorImager units into dCMP incorporation was performed as in Figure 6. The experiments were repeated three times, and the PhosphorImage of a representative experiment is shown.

extract-based repair synthesis, the K_m difference between the two forms of DNA may need to be taken into account.

In addition to characterizing rates of BER as a function of substrate form, we examined methods for analysis of repair patch length in the LP BER subpathway. Our initial experiments in this effort made use of phosphorothioate dNMP incorporation into the repair patch and subsequent exonuclease III digestion of products [data not shown, and ref. (37)]. This approach yielded spurious results (data not shown). The main difficulty stemmed from the capacity of exonuclease III to digest into the repair patches containing phosphorothioate dNMPs, leading to an underestimate of repair patch length. On the other hand, attempts to reduce the digestion strategically (time or enzyme concentration) generally lead to an over-estimate of repair patch length. Therefore, we concluded that reliable measurements of repair patch length could not be obtained with this approach. The approach described here, however, appeared to be reliable and was limited only by the technical requirements to obtain pure substrate preparations, restriction digestion of product

molecules to completion, and attention to accurate quantification of the amount of labeled dNMP incorporated.

REFERENCES

1. Klungland,A., Rosewell,I., Hollenbach,S., Larsen,E., Daly,G., Epe,B., Seeberg,E., Lindahl,T. and Barnes,D.E. (1999)

Accumulation of premutagenic DNA lesions in mice defective in removal of oxidative base damage. *Proc. Natl Acad. Sci. USA*, **96**, 13300–13305.

2. Lindahl,T. (1982) DNA repair enzymes. *Annu. Rev. Biochem.*, **51**, 61–87.

3. Lindahl,T. and Wood,R.D. (1999) Quality control by DNA repair. *Science*, **286**, 1897–1905.

4. Biade,S., Sobol,R.W., Wilson,S.H. and Matsumoto,Y. (1998) Impairment of proliferating cell nuclear antigen-dependent apurinic/apyrimidinic site repair on linear DNA. *J. Biol. Chem.*, **273**, 898–902.

5. Fortini,P., Pascucci,B., Parlanti,E., Sobol,R.W., Wilson,S.H. and Dogliotti,E. (1998) Different DNA polymerases are involved in the short- and long-patch base excision repair in mammalian cells. *Biochemistry*, **37**, 3575–3580.

6. Frosina,G., Fortini,P., Rossi,O., Carrozzino,F., Raspaglio,G., Cox,L.S., Lane,D.P., Abbondandolo,A. and Dogliotti,E. (1996) Two pathways for base excision repair in mammalian cells. *J. Biol. Chem.*, **271**, 9573–9578.

7. Klungland,A. and Lindahl,T. (1997) Second pathway for completion of human DNA base excision-repair: reconstitution with purified proteins and requirement for DNase IV (FEN1). *EMBO J.*, **16**, 3341–3348.

8. Dianov,G. and Lindahl,T. (1994) Reconstitution of the DNA base excision-repair pathway. *Curr. Biol.*, **4**, 1069–1076.

9. Horton,J.K., Prasad,R., Hou,E. and Wilson,S.H. (2000) Protection against methylation-induced cytotoxicity by DNA polymerase β-dependent long patch base excision repair. *J. Biol. Chem.*, **275**, 2211–2218.

10. Singhal,R.K., Prasad,R. and Wilson,S.H. (1995) DNA polymerase β conducts the gap-filling step in uracil-initiated base excision repair in a bovine testis nuclear extract. *J. Biol. Chem.*, **270**, 949–957.

11. Srivastava,D.K., Vande Berg,B.J., Prasad,R., Molina,J.T., Beard,W.A., Tomkinson,A.E. and Wilson,S.H. (1998) Mammalian abasic site base excision repair. Identification of the reaction sequence and rate-determining steps. *J. Biol. Chem.*, **273**, 21203–21209.

12. Podlutsky,A.J., Dianova,II, Podust,V.N., Bohr,V.A. and Dianov,G.L. (2001) Human DNA polymerase β initiates DNA synthesis during long-patch repair of reduced AP sites in DNA. *EMBO J.*, **20**, 1477–1482.

13. Sobol,R.W., Prasad,R., Evenski,A., Baker,A., Yang,X.P., Horton,J.K. and Wilson,S.H. (2000) The lyase activity of the DNA repair protein β-polymerase protects from DNA-damage-induced cytotoxicity. *Nature*, **405**, 807–810.

14. Sung,J.S., DeMott,M.S. and Demple,B. (2005) Long-patch base excision DNA repair of 2-deoxyribonolactone prevents the formation of DNA-protein cross-links with DNA polymerase β. *J. Biol. Chem.*, **280**, 39095–39103.

15. Albertella,M.R., Lau,A. and O'Connor,M.J. (2005) The over-expression of specialized DNA polymerases in cancer. *DNA Repair*, **4**, 583–593.

16. Canitrot,Y., Laurent,G., Astarie-Dequeker,C., Bordier,C., Cazaux,C. and Hoffmann,J.S. (2006) Enhanced expression and activity of DNA polymerase beta in chronic myelogenous leukemia. *Anticancer Res.*, **26**, 523–525.

17. Chen,K.H., Srivastava,D.K., Singhal,R.K., Jacob,S., Ahmed,A.E. and Wilson,S.H. (2000) Modulation of base excision repair by low density lipoprotein, oxidized low density lipoprotein and antioxidants in mouse monocytes. *Carcinogenesis*, **21**, 1017–1022.

18. Chen,K.H., Yakes,F.M., Srivastava,D.K., Singhal,R.K., Sobol,R.W., Horton,J.K., Van Houten,B. and Wilson,S.H. (1998) Up-regulation of base excision repair correlates with enhanced protection against a DNA damaging agent in mouse cell lines. *Nucleic Acids Res.*, **26**, 2001–2007.

19. Dong,Z.M., Zheng,N.G., Wu,J.L., Li,S.K. and Wang,Y.L. (2006) Difference in expression level and localization of DNA polymerase beta among human esophageal cancer focus, adjacent and corresponding normal tissues. *Dis Esophagus*, **19**, 172–176.

20. Srivastava,D.K., Rawson,T.Y., Showalter,S.D. and Wilson,S.H. (1995) Phorbol ester abrogates up-regulation of DNA polymerase β by DNA-alkylating agents in Chinese hamster ovary cells. *J. Biol. Chem.*, **270**, 16402–16408.

21. Harrigan,J.A., Wilson,D.M.3rd, Prasad,R., Opresko,P.L., Beck,G., May,A., Wilson,S.H. and Bohr,V.A. (2006) The Werner syndrome protein operates in base excision repair and cooperates with DNA polymerase β. *Nucleic Acids Res.*, **34**, 745–754.

22. Lavrik,O.I., Prasad,R., Sobol,R.W., Horton,J.K., Ackerman,E.J. and Wilson,S.H. (2001) Photoaffinity labeling of mouse fibroblast enzymes by a base excision repair intermediate. Evidence for the role of poly(ADP-ribose) polymerase-1 in DNA repair. *J. Biol. Chem.*, **276**, 25541–25548.

23. Matsumoto,Y., Kim,K., Hurwitz,J., Gary,R., Levin,D.S., Tomkinson,A.E. and Park,M.S. (1999) Reconstitution of proliferating cell nuclear antigen-dependent repair of apurinic/apyrimidinic sites with purified human proteins. *J. Biol. Chem.*, **274**, 33703–33708.

24. Prasad,R., Dianov,G.L., Bohr,V.A. and Wilson,S.H. (2000) FEN1 stimulation of DNA polymerase β mediates an excision step in mammalian long patch base excision repair. *J. Biol. Chem.*, **275**, 4460–4466.

25. Sobol,R.W., Horton,J.K., Kuhn,R., Gu,H., Singhal,R.K., Prasad,R., Rajewsky,K. and Wilson,S.H. (1996) Requirement of mammalian DNA polymerase-β in base-excision repair. *Nature*, **379**, 183–186.

26. Sandigursky,M., Freyer,G.A. and Franklin,W.A. (1998) The post-incision steps of the DNA base excision repair pathway in *Escherichia coli*: studies with a closed circular DNA substrate containing a single U:G base pair. *Nucleic Acids Res.*, **26**, 1282–1287.

27. Matsumoto,Y. (2001) Molecular mechanism of PCNA-dependent base excision repair. *Prog. Nucleic Acid Res. Mol. Biol.*, **68**, 129–138.

28. Wang,H. and Hays,J.B. (2000) Preparation of DNA substrates for in vitro mismatch repair. *Mol. Biotechnol.*, **15**, 97–104.

29. Wang,H. and Hays,J.B. (2001) Simple and rapid preparation of gapped plasmid DNA for incorporation of oligomers containing specific DNA lesions. *Mol. Biotechnol.*, **19**, 133–140.

30. Wang,H. and Hays,J.B. (2002) Mismatch repair in human nuclear extracts. Quantitative analyses of excision of nicked circular mismatched DNA substrates, constructed by a new technique employing synthetic oligonucleotides. *J. Biol. Chem.*, **277**, 26136–26142.

31. Beard,W.A. and Wilson,S.H. (1995) Purification and domain-mapping of mammalian DNA polymerase β. *Methods Enzymol.*, **262**, 98–107.

32. Slupphaug,G., Eftedal,I., Kavli,B., Bharati,S., Helle,N.M., Haug,T., Levine,D.W. and Krokan,H.E. (1995) Properties of a recombinant human uracil-DNA glycosylase from the UNG gene and evidence that UNG encodes the major uracil-DNA glycosylase. *Biochemistry*, **34**, 128–138.

33. Strauss,P.R., Beard,W.A., Patterson,T.A. and Wilson,S.H. (1997) Substrate binding by human apurinic/apyrimidinic endonuclease indicates a Briggs-Haldane mechanism. *J. Biol. Chem.*, **272**, 1302–1307.

34. Wang,Y.C., Burkhart,W.A., Mackey,Z.B., Moyer,M.B., Ramos,W., Husain,I., Chen,J., Besterman,J.M. and Tomkinson,A.E. (1994) Mammalian DNA ligase II is highly homologous with vaccinia DNA ligase. Identification of the DNA ligase II active site for enzyme-adenylate formation. *J. Biol. Chem.*, **269**, 31923–31928.

35. Carty,M.P., Lawrence,C.W. and Dixon,K. (1996) Complete replication of plasmid DNA containing a single UV-induced lesion in human cell extracts. *J. Biol. Chem.*, **271**, 9637–9647.

36. Widen,S.G. and Wilson,S.H. (1991) Mammalian beta-polymerase promoter: large-scale purification and properties of ATF/CREB palindrome binding protein from bovine testes. *Biochemistry*, **30**, 6296–6305.

37. Bennett,S.E., Sung,J.S. and Mosbaugh,D.W. (2001) Fidelity of uracil-initiated base excision DNA repair in DNA polymerase β-proficient and -deficient mouse embryonic fibroblast cell extracts. *J. Biol. Chem.*, **276**, 42588–42600.